Published in final edited form as:
Toxicol Appl Pharmacol. 2011 August 15; 255(1): 18–31. doi:10.1016/j.taap.2011.05.012.

Multi-Walled Carbon Nanotube-Induced Gene Expression in the Mouse Lung: Association with Lung Pathology

M Pacurari[1], **Y Qian**[2,*], **DW Porter**[2], **M Wolfarth**[2], **Y Wan**[1], **D Luo**[1], **M Ding**[2], **Castranova V**[1,2], and **NL Guo**[1,3,*]

[1] Mary Babb Randolph Cancer Center, West Virginia University, Morgantown, WV 26506-9300

[2] Pathology and Physiology Research Branch, Health Effects Laboratory Division, National Institute for Occupational Safety and Health, Morgantown, WV 26505

[3] Department of Community Medicine, School of Medicine, West Virginia University, Morgantown, WV 26506-9190

Abstract

Due to the fibrous shape and durability of multi-walled carbon nanotubes (MWCNT), concerns regarding their potential for producing environmental and human health risks, including carcinogenesis, have been raised. This study sought to investigate how previously identified lung cancer prognostic biomarkers and the related cancer signaling pathways are affected in the mouse lung following pharyngeal aspiration of well-dispersed MWCNT. A total of 63 identified lung cancer prognostic biomarker genes and major signaling biomarker genes were analyzed in mouse lungs (n = 80) exposed to 0, 10, 20, 40, or 80 μg of MWCNT by pharyngeal aspiration at 7 and 56 days post-exposure using quantitative PCR assays. At 7 and 56 days post-exposure, a set of 7 genes and a set of 11 genes, respectively, showed differential expression in the lungs of mice exposed to MWCNT vs. the control group. Additionally, these significant genes could separate the control group from the treated group over the time series in a hierarchical gene clustering analysis. Furthermore, 4 genes from these two sets of significant genes, coiled-coil domain containing-99 *(Ccdc99)*, muscle segment homeobox gene-2 *(Msx2)*, nitric oxide synthase-2 *(Nos2)*, and wingless-type inhibitory factor-1 (*Wif1)*, showed significant mRNA expression perturbations at both time points. It was also found that the expression changes of these 4 overlapping genes at 7 days post-exposure were attenuated at 56 days post-exposure. Ingenuity Pathway Analysis (IPA) found that several carcinogenic-related signaling pathways and carcinogenesis itself were associated with both the 7 and 11 gene signatures. Taken together, this study identifies that MWCNT exposure affects a subset of lung cancer biomarkers in mouse lungs.

Keywords

Nanoparticles; Lung cancer; Biomarker; Gene expression; Molecular network analysis

[*]Corresponding authors: Nancy L. Guo, Mary Babb Randolph Cancer Center and Department of Community Medicine, West Virginia University, Morgantown, WV 26506-9300, Tel: (304) 293-6455; Fax: (304) 293-4667;, lguo@hsc.wvu.edu, and, Yong Qian, Pathology and Physiology Research Branch, Health Effects Laboratory Division, National Institute for Occupational Safety and Health, 1095 Willowdale Road, Morgantown, WV 26505-2888, Tel: (304) 285-6286; Fax: (304) 285-5938;, yaq2@cdc.gov.

Introduction

Carbon nanotubes (CNT) represent an important class of engineered nanomaterials. They can be synthesized either as single-walled carbon nanotubes (SWCNT) or as multi-walled carbon nanotubes (MWCNT). SWCNT consist of a single sheet of graphite rolled-up in the form of a cylinder with a diameter of 1–2 nm and lengths ranging up to several micrometers. MWCNT consist of several stacked single wall carbon nanotubes with diameters up to 100 nm and lengths up to several micrometers (Pacurari *et al.*, 2010). Due to their unique physicochemical properties, MWCNT have been widely used for various industrial applications, including, but not limited to, supercapacitors, batteries, automotive industry, aerospace industry, electronics, pharmaceutics, bio-engineering, medical devices, and biomedicine (Pacurari *et al.*, 2010).

Concern over potential MWCNT-induced toxicity has emerged, particularly due to the structural similarity between asbestos and MWCNT. Asbestos is a group of naturally occurring hydrated silicate minerals with fibrous morphology (Pacurari *et al.*, 2010). They consist of fibers of various lengths and diameters, with lengths ranging from 0.1 to greater than 200 μm. It has been well known that asbestos exposure leads to the development of pulmonary fibrosis (asbestosis), bronchogenic lung cancer, pleural plaques, and malignant mesothelioma (Pacurari *et al.*, 2010). Numerous studies have demonstrated that fiber length, diameter, and durability are critical factors involved in the pathogenicity of asbestos (Pacurari *et al.*, 2010). Although MWCNT have a tendency to bundle together, MWCNT aerosols may contain many long, thin, fiber-like nanotube structures similar to asbestos (Pacurari *et al.*, 2010). In addition, the resistance of MWCNT to high temperature or acid treatment indicates that these engineered fibers are durable. It has been proposed that these unique asbestos-like properties of MWCNT may potentially induce pathogenic and carcinogenic effects (Service, 1999; Donaldson *et al.*, 2006; Tian *et al.*, 2006). Indeed, several studies reported that MWCNT induce inflammation, granuloma formation, and biopersistence in the rodent lung after 60 days post-exposure (Muller *et al.*, 2005; Elgrabli *et al.*, 2008; Porter *et al.*, 2010). Other studies have shown that MWCNT exposure increases the genotoxic potential both in vivo and in vitro (Muller *et al.*, 2008).

Recently, our group conducted an in vivo dose-response and time course study of MWCNT exposure in mice in order to investigate the ability of MWCNT to induce pulmonary inflammation, damage, and fibrosis (Porter *et al.*, 2010). Mice were exposed to 0, 10, 20, 40, or 80 μg of MWCNT by pharyngeal aspiration. At 1, 7, 28, and 56 days post-exposure, MWCNT-induced pulmonary toxicity was evaluated. The results demonstrate that pulmonary inflammation and damage were dose-dependent, appeared 1 day post-exposure, and peaked 7 days post-exposure. In contrast, morphometric analysis of lung tissue from this study by Mercer et al. (Mercer *et al*., 2011) indicates that MWCNT-induced interstitial fibrosis increased at day 28 and progressed through 56 days post-exposure. These results indicate that MWCNT exposure rapidly produces significant pulmonary inflammation, damage, and fibrosis.

Several studies have indicated that fibrosis, a pulmonary fibrotic scarring, could be a precursor to lung cancer. A clinical study found that lung scarring was associated with elevated lung cancer risk, and furthermore, they found that pulmonary scarring and lung cancer occurred to the same lung and extended over time (Yu *et al.*, 2008). In a review over a 21 year period of lung cancer patients, it was found that 45% of all peripheral lung cancers originated in a lung scar (Auerbach *et al.*, 1979). A study with computed tomographic (CT) scans and pathologic specimen analysis found that 47 patients of 57 histologically proved lung cancers had pulmonary fibrosis, indicating a possible association between lung cancer and fibrosis (Sakai *et al.*, 2003).

A casual relationship between lung fibrosis and lung cancer has been observed in crystalline silica exposed patients. Literature review indicated that an increased risk of lung cancer among patients with silicosis, a progressive lung fibrosis, might be an effect of the lung fibrosis rather than a direct effect of silica exposure (Peretz *et al.*, 2006). Analysis of the relationship between tuberculosis-induced lung fibrosis and lung cancer indicated that there is an association between tuberculosis and increased lung cancer risk (Shiels *et al.*, 2011), which implicates chronic pulmonary scarring in the etiology of lung cancer.

One study indicated that pulmonary fibrosis may not be a precursor for lung cancer, rather it may increase the susceptibility of fibrosis patients to develop a lung cancer over time. A comparative study of metaplastic epithelia in lungs of usual interstitial pneumonia (UIP), idiopathic pulmonary fibrosis, with or without lung cancer showed that 32 of 70 UIP autopsy cases had lung cancer, and quantitative assessment of the metaplastic epithelia in lungs demonstrated that squamous metaplasia occurred more frequently in UIP with lung cancer than in UIP without lung cancer (Hironaka and Fukayama, 1999).

Molecular biological analysis also supports that lung fibrosis and lung cancer could be associated. Immunohistochemical analysis found that TGF-beta expression is increased in asbestos-induced fibrosis (Jagirdar *et al.*, 1997). TGF-beta is a ubiquitous and essential regulator of cellular proliferation, differentiation, migration, cell survival, and angiogenesis (Elliott and Blobe, 2005). Alterations in the TGF-beta have been associated with human cancers, including lung cancer. TGF-beta signaling promotes epithelial to mesenchymal transition, a process by which cells lose their epithelial characteristics and acquire more migratory and metastatic mesenchymal properties (Toonkel *et al.*, 2010). An increase in TGF-beta expression in fibrosis may imply that fibrotic scarring may increase the risk of carcinogenesis. Several biological and pathological characteristics of lung fibrosis are similar to that of lung cancer, including genetic alterations, uncontrolled proliferation, and tissue invasion (MacKinnon *et al.*, 2010; Vancheri *et al.*, 2010).

Although more research is needed for the assessment of the clinical outcome of lung fibrosis, Vancheri et al. (Vancheri *et al.*, 2010) suggested that the abnormal fibroblast proliferation observed in idiopathic pulmonary fibrosis may be associated with the development of lung cancer. The current study was designed to follow up our previous investigation of MWCNT-induced pulmonary inflammation, damage, and fibrosis in the mouse. The aim of this study was to successfully profile MWCNT-induced gene expression changes within a set of previously identified lung cancer biomarkers (Guo *et al.*, 2006; Guo *et al.*, 2008) using MWCNT-exposed mouse lungs from a previous study (Porter *et al.*, 2010). Ultimately, the association between MWCNT-induced pulmonary inflammation, damage and fibrosis and genetic markers for lung carcinogenesis was investigated.

In our previous lung cancer-related genome-wide DNA microarray analysis, a 35-gene signature was identified from 86 lung adenocarcinoma patients in order to predict tumor recurrence (Guo *et al.*, 2006). This 35-gene prognostic signature was further validated in 348 non-small cell lung cancer (NSCLC) patients using their transcriptional profiles generated from microarray studies (Guo *et al.*, 2008). The gene expression of the 35 biomarkers was confirmed with real-time RT-PCR analysis of independent snap-frozen human lung cancer tumors (Guo *et al.*, 2008). In the Director's Challenge Study, a separate set of patient cohorts from multiple hospitals was analyzed, and a new 12-gene signature was identified from genome-wide DNA microarray analysis. This 12-gene signature provides accurate prognostic stratification of 442 lung adenocarcinoma patients including those with early stage tumors (Wan *et al.*, 2010). We hypothesize that expression profiling of lung cancer biomarkers in MWCNT-exposed mouse lungs will identify a subset of biomarkers affected by the exposure, suggesting a possible association between MWCNT

exposure and lung cancer risk. These biomarkers could be relevant for early detection or medical surveillance of lung cancer risk in occupationally-exposed workers. In the current study, in order to identify biomarkers relevant for risk prediction of lung carcinogenesis after MWCNT exposure, quantitative RT-PCR low density arrays (LDA) were designed to measure the gene expression profiles of the identified 47 lung cancer prognostic markers (Guo *et al.*, 2006; Guo *et al.*, 2008; Wan *et al.*, 2010) as well as several major signaling transduction pathway genes in lung tissues from mice exposed to different doses of MWCNT at 7 and 56 days post-exposure (Table 1).

Materials and Methods

MWCNT

MWCNT used in this study were a gift from Mitsui-&-Company (MWCNT-7, lot # 05072001K28). The characterization of MWCNT has been published (Porter *et al.*, 2010). Briefly, the bulk MWCNT exhibit a distinctive crystalline structure with the number of walls ranging from 20 to 50 walls. Overall, MWCNT trace metal contamination was 0.78%, including sodium (0.41%) and iron (0.32%) with no other metals present above 0.02%. Transmission electron microscopy (TEM) micrographs of MWCNT dispersed in dispersion medium (DM) demonstrated that DM promotes significant dispersion of MWCNT. The quantitative analysis of TEM micrographs revealed that the median length of this MWCNT sample was 3.86 μm (GSD 1.94) and the count mean width was 49 ±13.4 (S.D.) nm. The zeta potential of the MWCNT in the DM was determined to be −11mV.

Animals

Male C57BL/6J mice (7 weeks old) were obtained from Jackson Laboratories (Bar Harbor, ME). Since male mice fight and injury each other if caged together, individual mice were housed one per cage in polycarbonate isolator ventilated cages, which were provided HEPA-filtered air, with fluorescent lighting from 0700 to 1900 hours. Autoclaved Alpha-Dri virgin cellulose chips and hardwood Beta-chips were used as bedding. Mice were monitored to be free of endogenous viral pathogens, parasites, mycoplasms, Helicobacter and CAR Bacillus. Mice were maintained on Harlan Teklad Rodent Diet 7913 (Indianapolis, IN), and tap water was provided ad libitum. Animals were allowed to acclimate for at least 5 days before use. All animals used in this study were housed in an AAALAC-accredited, specific pathogen-free, environmentally controlled facility.

MWCNT pharyngeal aspiration exposure

Suspensions of MWCNT were prepared in DM as previously described by our laboratory (Porter *et al.*, 2008). Each treatment group consisted of 8 mice. Mice were anesthetized with isoflurane (Abbott Laboratories, North Chicago, IL). When fully anesthetized, the mouse was positioned with its back against a slant board and suspended by the incisor teeth using a rubber band. The mouth was opened, and the tongue gently pulled aside from the oral cavity. A 50μl aliquot of sample was pipetted at the base of the tongue, and the tongue was restrained until at least 2 deep breaths were completed (but for not longer than 15 seconds). Following release of the tongue, the mouse was gently lifted off the board, placed on its left side, and monitored for recovery from anaesthesia. Mice received either DM (vehicle control), 10, 20, 40 or 80 μg MWCNT.

RNA extraction

Total RNA was extracted from the frozen mouse lung tissue sample (−80 °C) in RNAlater using the RNeasy Fibrous Tissue Mini Kit according to the manufacturer's protocol (Qiagen, USA). Total RNA was eluted in RNase-free water and stored at −80°C until further

analysis. The quality and the concentration of each RNA sample was determined using a Nanodrop-1000 Spectrophotometer (NanoDrop Tech, Germany).

Quantitative real-time PCR (qPCR)

cDNA was generated using a TaqMan high capacity RT kit according to manufacturer's protocol (Applied Biosystems, CA). Real-time qPCR was performed using TaqMan microfluidic low density arrays (LDA) with custom designed genes on an ABI 7900HT Fast RT-PCR instrument (Applied Biosystems). The reports were generated using SDS2.3 software (Applied Biosystems), and the expression level of each gene was given by the number of cycles required to reach threshold fluorescence (*Ct*). 18S was used as an endogenous control gene.

Statistical analysis

At every time point measured, each treatment and control group consisted of eight mice. To assess the gene expression fold change in each treated group versus the control group, the gene expression (*Ct* value) of three replicates was first averaged for each sample. Second, each gene expression value was normalized using the average expression of 18S for the entire plate, i.e. plate-wise normalization. Third, the fold change between treatment groups versus the control group was calculated using $2^{-\Delta\Delta Ct}$ method (Livak and Schmittgen, 2001). Finally, the statistical significance was assessed with two-sample *t*-tests using software SAS 9.2. In order to assess post-exposure effects over the time series, a two-sample *t*-test was also performed on the fold change values between two time points for each gene.

Functional Pathway Analysis

Ingenuity Pathway Analysis (IPA) software (Ingenuity Systems, Redwood City, CA) was used to derive curated molecular interactions reported in the literature. These interactions included both physical and functional interactions, as well as interactions representing pathway relevance. In this study, in order to delineate molecular networks of genes interacting with the 7-gene or 11-gene biomarker sets, a core analysis was employed to identify the most significant biological functions and processes from the derived interactions reported in mouse studies with IPA. The statistical significance of canonical signaling pathways and associated disease and disorder functions were assessed using *Fisher*'s exact tests adjusted with BH tests.

Hierarchical clustering analysis and heatmap

Hierarchical two-dimensional clustering analysis was performed using genes that exhibited significant differential expression after treatment at 7 and 56 days post-exposure, using the *Heatplus* function in the *R* package. Similarity metrics were *manhattan* distance, and the cluster method was complete linkage. Heatmaps were then generated in the *R* package.

Results

A 7-gene biomarker set identified at 7 days post-exposure

A total of 63 lung cancer prognostic and major signaling pathway biomarker genes were analyzed using qPCR assays in mouse lungs exposed by aspiration to 0, 10, 20, 40, or 80 μg of MWCNT at 7 days post-exposure. Overall, it was found that only 7 genes had different expression levels compared to the control group. These 7 genes were Rho GTPase activating protein-19 (*Arhgap19)*, coiled-coil domain containing-99 (*Ccdc99*), muscle segment homeobox gene-2 (*Msx2*), methalothione-3 *(Mt3),* nitric oxide synthase-2 *(Nos2),* sonic hedgehog homolog *(Shh),* and wingless-type inhibitory factor-1 (*Wif1)*. The expression levels of *Arhgap19*, *Msx2*, and *Shh* were significantly increased only at the exposure dose of

40 μg MWCNT. The expression level of *Wif1* was found to be significantly decreased only at the dose of 80 μg MWCNT exposure. The expression levels of *Ccdc99* and *Nos2* were significantly increased at doses of 20, 40, and 80 μg of MWCNT, whereas the expression of *Mt3* was significantly increased at doses of 40 and 80 μg of MWCNT (Figure 1). These results indicate that several lung cancer biomarker signature genes are affected during the earlier stage of MWCNT exposure.

An 11-gene biomarker set identified at 56 days post-exposure

qRT-PCR analysis was applied to assess the expression changes of 63 lung cancer prognostic and major signaling biomarker genes in mouse lungs exposed by aspiration to 0, 10, 20, 40, or 80 μg of MWCNT at 56 days after a single exposure. At 56 days post-exposure, it was found overall that 11 genes exhibited differential expression levels compared to the control group (Figure 2). These 11 genes were B-cell leukemia/ lymphoma-2 (*Bcl2)*, caveolin-1 *(Cav1)*, *Ccdc9*, desert hedgehog homolog *(Dhh)*, gluthatione peroxidase-3 *(Gpx3)*, *Msx2*, *Nos2*, phosphatidylinositol 3-kinase regulatory subunit-1 (*Pi3kr1)*, patched-1 *(Ptch1)*, *Wif1*, and leucine-zipper and sterile-alpha motif kinase (*Zak*) (Figure 2). Of these 11 genes, eight genes, *Bcl2*, *Cav1*, *Dhh*, *Gpx3*, *Pi3kr1*, *Ptch1*, *Zak*, and *Wif1*, had a significant decreased expression level at the highest tested dose (80 μg). The expression of *Msx2* exhibited significant decreases at the doses of 20 and 80 μg. In contrast, *Nos2* expression level was significantly increased at the doses of 10 and 80 μg. *Ccdc99* expression was significantly increased at 40 μg of MWCNT (Figure 2). These results indicate that after 56 days post-exposure to MWCNT, the expression levels of several lung cancer biomarkers have differential expression levels compared to control samples.

A common 4-gene biomarker set between 7 and 56 days post-exposure

Further analysis found that 4 genes appeared in the gene biomarker sets for both the 7-and 56 days post-exposure samples. These four overlapping genes were *Ccdc99*, *Msx2*, *Nos2*, and *Wif1* (Figure 3). A comparison of the expression of these overlapping genes between 7 days (7-gene set) and 56 days (11-gene set) post-exposure samples revealed that the expression of three genes, *Ccdc99*, *Nos2* and *Msx2*, decreased at 56 days post-exposure compared to their expression at 7 days post-exposure (Figure 3A-C). Statistical analysis demonstrated that the expression levels of *Ccdc99* and *Nos2* at 7 days were significantly higher compared with those at 56 days post-exposure (Figure 3A, 3C). These results further indicate that the expression of selected lung cancer biomarkers show differential expression levels during the more extended post-exposure interval.

Gene clustering analysis

Hierarchical clustering analysis showed that the 7-gene biomarker set was able to separate MWCNT-treated animals from the control animals at 7 days post-exposure (Figure 4A). The 7-gene biomarker set showed elevated gene expression in the treated animals, except for *Wif1* (Figure 4A and Figure 1). At 56 days post-exposure, the expression pattern of the 11-gene biomarker set was not as homogenous among the MWCNT-treated animals compared with that at 7 days post-exposure (Figure 4B). Most genes exhibited decreased expression in the majority of MWCNT-exposed animals compared with a middle cluster containing four vehicle control-exposed animals (marked in Figure 4B).

Molecular network analysis

To investigate significant molecular network interactions and canonical signaling pathways associated with these differentially expressed genes, the Ingenuity Pathway Analysis (IPA) software was applied to analyze 7- and 11-gene biomarker sets, respectively. The results revealed that a total of 25 and 60 genes interacted with 7- and 11-gene biomarker sets,

respectively (Figure 5). The analysis also demonstrated that 25 canonical pathways were associated with the 7-gene biomarker set. Among these 25 pathways, 13 were statistically significant ($p<0.05$). Ranking the pathways by their significance, the top five most significant were: corticotrophin releasing hormone signaling, the role of macrophages, fibroblasts and endothelial cells in rheumatoid arthritis, sonic hedgehog signaling, MIF regulation of innate immunity and MSP-RON signaling pathway (Figure 6A). For the 11-gene biomarker set, 154 associated canonical pathways were identified. Among these 154 pathways, 81 were statistically significant ($p<0.05$). Based on the ranking of the significance, the top five most significant pathways were: molecular mechanisms of cancer, docosahexaenoic acid (DHA) signaling, the role of osteoblasts, osteoclasts and chondrocytes in rheumatoid arthritis, MSP-RON signaling pathway and glucocorticoid receptor signaling (Figure 6B). Notably, the molecular mechanisms of cancer pathway was ranked as the most significant among the 11-gene associated canonical pathways at 56 days post-exposure.

The IPA also identified 12 common canonical pathways between the 7- and 11-gene biomarker sets. Notably, basal cell carcinoma signaling pathway was ranked as the most significant among these 12 overlapping pathways (Figure 6C). An analysis of the 7- and 11-gene biomarker sets-associated potential diseases and biological function disorders showed that carcinogenesis was ranked fifth among the 7-gene set-associated diseases and function disorders (at 7 days post-exposure). For the 11-gene set network (at 56 days post exposure), carcinogenesis was ranked thesecond most significant disease function (Figure 6D). Taken together, these results indicate that exposure to MWCNT may be potentially carcinogenic in humans, which could be enhanced over a prolonged post-exposure period.

Discussion

Several studies have demonstrated that exposure to CNT substantially induces harmful effects on the lungs, including inflammatory granulomas and lung fibrosis in animal models (Lam *et al.*, 2004; Muller *et al.*, 2005; Shvedova *et al.*, 2005; Porter *et al.*, 2010). Furthermore, it has been proposed that CNT exposure can induce an asbestos-like pathogenicity and may pose a similar carcinogenic risk as exposure to asbestos fiber does (Takita *et al.*, 1986; Donaldson *et al.*, 2006; Poland *et al.*, 2008). In fact, MWCNT are man-made fiber-shaped materials. The concern of their potential health hazards has been raised due to their unique physical properties, such as high aspect ratio (length/diameter), nanoscale diameters, micrometer length fiber like-shape and durability, which are analogous to asbestos fibers (Muller *et al.*, 2005; Donaldson *et al.*, 2006; Kobayashi *et al.*, 2010). Particularly, the high aspect ratio and micrometer length are two important features that may contribute to the fiber toxicity (Stanton *et al.*, 1981). Whether MWCNT fit the classical fiber 'paradigm' has not yet been fully established. Poland et al. (Poland *et al.*, 2008) reported an asbestos-like acute inflammatory effect of long MWCNT when they were administered into abdominal cavity of mice. They found that the asbestos-like effects were fiber length-dependent since results showed that short fibers failed to induce abdominal inflammation or granulomas. Conversely, long fibers induced inflammation and granulomas at the peritoneal side of the diaphragm at 24 h and 7 days post-exposure. Another study by Takagi et al. (Takagi *et al.*, 2008) reported that intra-abdominal exposure to MWCNT induced mesothelioma, a form of cancer of the lining of the body cavities, in $p53^{+/-}$ mice. In this study, the $p53^{+/-}$ mouse was chosen because it is sensitive to induction of tumors. Histopathological analysis of the peritoneal cavity of MWCNT-treated $p53^{+/-}$ mice found the presence of several asbestos-like pathological changes, such as fibrous scars, granulomas, and typical epithelial mesotheliomas. Particularly, the characteristics of MWCNT-induced mesotheliomas were hobnail appearance to large tumors along with high mitotic rate cells and central necrosis due to high grade of malignant mesothelioma. Furthermore, recent two studies show that MWCNT can reach the pleural tissue in mice, the

site of mesothelioma, after pulmonary exposure to occupationally relevant burdens of MWCNT (Ryman-Rasmussen *et al.*, 2009; Mercer *et al.*, 2010) These studies conclude that the fibrous structure of MWCNT may pose a carcinogenic risk similar to that for asbestos fibers.

It has been well-established that the biopersistence and pulmonary penetration potential of asbestos are the critical factors associated with asbestos pathogenicity and carcinogenicity (Vallyathan *et al.*, 1998; Shukla *et al.*, 2003). Studies have shown that MWCNT exposure has a similar pattern of biopersistence and pulmonary penetration as asbestos (Elgrabli *et al.*, 2008; Kim *et al.*, 2010). Recent studies found that MWCNT were persistent in lungs up to 60 days post-exposure (Muller *et al.*, 2005; Porter *et al.*, 2010). In addition, histopathological analyses found that upon pulmonary exposure to MWCNT the particles penetrated through alveolar walls and were transported to the alveolar interstitium, subpleural tissue and subpleural lymphatics, finally reaching the intrapleural space (Porter *et al.*, 2010).

Several in vitro studies have shown that MWCNT exposure induces genotoxicity. Zhu et al. (Zhu *et al.*, 2007) found that MWCNT exposure induces DNA damage and increases mutation frequency in mouse embryonic stem cells. Karlsson et al.(Karlsson *et al.*, 2008) demonstrated that MWCNT exposure significantly damages DNA in A549 type II epithelial cells. Sargent et al. (Sargent *et al.*, 2011) found that MWCNT induce mitotic abnormality with one mitotic spindle pole, showing the evidence of the mechanism responsible for the disruption of cell division by MWCNT. Their results indicate that MWCNT are genotoxic, which may result in carcinogenic potential for MWCNT. These results are in agreement with our present results of MWCNT-induced lung cancer biomarker gene expression changes. Although whether MWCNT would induce tumors can't be addressed in the present study, our data indicate an association between MWCNT exposure and lung cancer biomarker changes. Such an association has been used to justify a current project within NIOSH to evaluate lung tumor formation over the course of 1 year after a 2 week inhalation of MWCNT in a cancer susceptible mouse strain.

Taken together, the fibrous characteristics of MWCNT, their biopersistence, their ability to penetrate the lungs, and their genotoxicity have prompted the hypothesis that exposure to MWCNT may contribute to the initiation and progression of asbestos-like pathological responses, such as lung carcinogenesis (Donaldson *et al.*, 2006; Pacurari *et al.*, 2010).

In the present study, we sought to determine whether MWCNT exposure would affect lung cancer biomarker gene expression through profiling a set of lung cancer biomarker genes in mouse lungs following exposure to MWCNT. The design of this study was established based on our previous in vivo mouse model for pharyngeal aspiration of MWCNT (Porter *et al.*, 2010). The mouse lung tissue specimens at both 7 and 56 days post-MWCNT exposure were taken from this previous investigation and were analyzed for the expression changes of a set of 63 lung cancer biomarker genes using RT-PCR analysis (Table 1). Of these 63 genes, 47 were previously shown to be prognostic markers of human lung cancer recurrence and metastasis (Guo *et al.*, 2006; Guo *et al.*, 2008; Wan *et al.*, 2010), and the remaining 16 genes are well established hallmarks of cancer signaling pathways. The 47 lung cancer prognostic biomarkers were from a 35-gene (Guo *et al.*, 2006) and a 12-gene signature (Guo *et al.*, 2008), respectively. Both lung cancer gene signatures could identify more aggressive tumors from stage I non-small cell lung cancer tumors, which were at the early stage of cancer formation by the time of diagnosis. We have data showing that 45 out of 47 prognostic markers were also significantly differentially expressed in NSCLC tumors vs. normal lung tissues (currently unpublished results). Specifically, *Msx2* and *Ccdc99* were both over-expressed in lung cancer tumor tissues with a fold change of 2.3 and 1.8,

respectively, which are concordant with the over-expression patterns observed in the MWCNT-treated mouse lungs in this study. The functions of these 63 genes and the associated signaling transduction pathways were extracted from the literatures and are listed in Table 1.

The results obtained from our study demonstrated that 7 genes out of these 63 lung cancer biomarker genes showed differential expression changes at 7 days post-exposure to MWCNT. These 7 genes are *Arpgap19, Nos2, Shh, Wif1, Mt3, Ccdc99,* and *Msx2.* The functional analysis of 7 genes showed that: 1) *Arpgap19, Nos2, Shh,* and *Wif1* are involved in signaling transduction, 2) *Mt3* is involved in metal detoxification, cell proliferation, and cell protection against damage, 3) *Ccdc99* is involved in cell cycle regulation, and 4) *Msx2* is a transcription factor and an oncogene (Table 1). Particularly, *Shh,* a tissue developmental and angiogenic factor, is involved in tumor angiogenesis in a variety of cancers, and *Mt3,* modulated by oxidative stress, plays a role in carcinogenesis (Pola *et al.,* 2001; Garrett *et al.,* 2002). The increase in expression of both genes upon MWCNT exposure in mouse lungs may indicate the potential molecular mechanisms related to MWCNT-induced potential carcinogenic effects. Such a relationship warrants further study.

At 56 days post-exposure to MWCNT, the gene profiling showed that 11 genes underwent different expression changes. These 11 genes are: *Dhh, Nos2, Ptch1, Pik3r1, Zak, Wif1, Ccdc99, Cav1, Bcl2, Msx2,* and *Gpx3*. The functional analysis of these 11 genes showed that: 1) *Dhh, Nos2, Ptch1, Pik3r1, Zak,* and *Wif1* are involved in signaling transduction, 2) *Ccdc99* is a cell cycle protein, 3) *Cav1* is associated with plasma membrane, 4) *Bcl2* is an anti-apoptotic gene, 5) *Msx2* is a transcription factor and an oncogene, and 6) *Gpx3* is involved in antioxidant activity (Table 1). Notably, *Bcl2* is an anti-apoptotic gene and plays a major role in tumorigenesis (Coultas and Strasser, 2003). The decrease in *Bcl-2* gene expression in this study indicates that MWCNT exposure may damage anti-oncogenic suppressor genes in mouse lungs.

Furthermore, these two sets of significant genes at 7 and 56 days post-exposure share 4 common genes between them. These genes are: *Ccdc99, Msx2, Nos2,* and *Wif1* (Figure 3). The data analysis showed that the expression changes of these 4 overlapping genes at 7 days post-exposure were attenuated at 56 days post-exposure. Interestingly, our previous in vivo studies have shown that MWCNT-induced pulmonary inflammation and damage peaked at 7 days post-exposure of MWCNT (Porter *et al.*, 2010); while interstitial fibrosis was significantly elevated at 28 days post-exposure and peaked at 56 days (Mercer *et al.,* 2011). Therefore, the time-dependent changes in gene expression profiling correlate with the previously published results of histopathological measurements in mouse lungs, indicating a transient inflammatory/damage response and persistent fibrosis. These results demonstrate that gene profiling may well reveal alterations in the molecular processes at the level of the gene transcription and signaling transduction pathways upon MWCNT exposure in mouse lungs.

The notion of predicting chemical toxicity by gene expression profiling has been proposed and applied in genotoxicity for several decades (Aubrecht and Caba, 2005). Particularly, the recent development of high-throughput technologies has made it possible to identify key predictive biomarkers through global gene expression profiling. It has become increasingly important to use gene expression signatures identified with bioinformatics methods for toxicity predication (Shi *et al.,* 2010), risk assessment, and screening (Afshari *et al.*, 2011). A similar gene expression and copy number profiling study was conducted to identify important allelic imbalance in asbestos-related lung cancer (Wikman *et al.,* 2007). Blood gene expression signatures have been used to predict exposure levels of APAP (Bushel *et al.,* 2007). The unique advantage of these studies, as well our present study, is the ability to

detect toxic injury at the molecular level and to identify the signaling pathways that lead to organ injury long before the clinical symptoms occur. In these biomarker and gene signature studies, the emphasis is on the prediction of potential risk or toxicity. In this study, the lung tissues were collected from the mice at 7 and 56 days post-exposure, which are not long enough for mice to develop lung cancer. In the case of asbestos exposure, the latency period between the first exposure and diagnosis of mesothelioma ranges from 20 to 40 years (Pacurari *et al.*, 2010). An in vivo animal study demonstrated that asbestos exposure induces malignant mesothelioma in mouse lungs at 60 weeks post-exposure (Vaslet *et al.*, 2002). Thus, neither asbestos nor MWCNT would be able to induce lung carcinogenesis in mice at 56 days post-exposure. In vivo animal model-generated gene profiling reveals information that approximates the complexity of the human body and its cellular, biochemical, and molecular systems that are involved in responses to chemical agents. Several studies have shown that animal model-based gene expression profiling can predict human target organ toxicities reliably for numerous human diseases, including cancer (Nuwaysir *et al.*, 1999; Newton *et al.*, 2004). The combined results from the gene expression profiling in this study and the histopathological changes observed in the previous study (Porter *et al.*, 2010) indicate that exposure to MWCNT may potentially enhance the risk of pulmonary diseases, including lung carcinogenesis, in humans. Thus, results from the present study have been used to justify a further investigation by NIOSH to address whether the changes observed in gene expression in lung target cells are involved in the pathogenesis of lung cancer. Specifically, NIOSH is currently conducting a two week inhalation exposure study with histological evaluation through 1 year post-exposure in a cancer susceptible mouse strain.

Ingenuity Pathway Analysis (IPA) software analyzes the gene information from more than 200,000 published full text articles in order to create global gene networks, an interactome. At the same time, IPA relates specific biological functions and potential diseases and functional disorders to individual genes (Calvano *et al.*, 2005; Long *et al.*, 2008). The software is used to identify significant networks, biological functions, potential diseases and canonical signaling pathways associated with the differentially expressed gene profiles. The results obtained from IPA show a correlation between our gene expression profiling and an empirical classification of biological functions and potential diseases. Among the top five most significant canonical pathways associated with the 7-gene biomarker set, 4 pathways (corticotrophin releasing hormone signaling, Sonic hedgehog signaling, MIF regulation of innate immunity, and MSP-RON signaling pathway) are involved in carcinogenesis. Furthermore, the results of IPA showed that cancer is one of top 5 diseases and functional disorders associated with the 7-gene biomarker set. Similarly, 4 out of the 5 most significant canonical pathways associated with 11-gene biomarker set are involved in carcinogenesis and cancer is ranked as the second most significant of the potential diseases and functional disorders listed. Moreover, the comparison of results from analyses of both gene sets showed that there are 12 overlapping significant canonical signaling pathways and that basal cell carcinoma signaling is ranked as the most significant pathway.

Our IPA results also showed that MWCNT induced potentially carcinogenic alterations in the genes of mice and that these changes were time dependent. The Signaling Pathway of Molecular Mechanisms of Cancer is ranked as the most significant among the 11-gene biomarker set-associated canonical pathways at 56 days post-exposure. Notably, it is ranked much lower among the 7-gene biomarker set-associated canonical pathways at 7 days post-exposure. Furthermore, cancer is ranked as thesecond most significant among the 11-gene set-associated diseases and functional disorders whereas in the 7-gene set analysis, its significance falls to the fifth. These results are consistent with those of our histopathological measurements (Porter *et al.*, 2010; Mercer *et al.*, 2011). They demonstrate a shift from rapid/transient inflammation/damage to a persistent fibrotic response involving remodeling signals

and growth factor damages, and as well as epithelial hyperplasia and hypertrophy (Porter *et al.*, 2010). Such changes have been associated with initiation of carcinogenesis.

The IPA results were focused on the 7- and 11-gene sets identified in this study. As only cancer-related genes were initially analyzed in the experiments, the results would be biased toward cancer related pathways and functions, as opposed to those obtained from genome-wide expression studies. However, the identified biomarkers are involved in multiple diseases. Pathological disorders, such as organismal disorders and injuries (including fibrosis), were also retrieved from the IPA database as significant functions, indicating that the genes identified in this study were associated with the observed MWCNT-induced lung pathology.

Overall, the results obtained from this study have demonstrated that MWCNT exposure induces changes in lung cancer biomarker gene expression in mouse lungs, which may indicate a potential association between MWCNT exposure-induced lung inflammatory, damage and fibrotic responses and lung carcinogenesis. The results of the IPA also indicate that MWCNT exposure may induce alterations in several disease-related signaling transduction pathways. In light of this finding, long term inhalation studies of MWCNT to monitor possible induction of lung tumors and/or mesothelioma are justified. NIOSH is currently conducting a two week inhalation exposure to MWCNT in a cancer susceptible mouse strain with histological evaluation through 1 year post-exposure to address this issue. Additionally, the results obtained from this study indicate these gene signature alterations of MWCNT exposure and could conceivably be used for the medical surveillance of occupationally-exposed MWCNT workers.

Acknowledgments

We thank Rebecca Raese for her help in editing the manuscript. This study is supported by NIH/NLM R01LM009500 (PI: Guo) and NCRR P20RR16440 and Supplement (PD: Guo).

References

Afshari CA, Hamadeh HK, Bushel PR. The Evolution of Bioinformatics in Toxicology: Advancing Toxicogenomics. Toxicological Sciences. 2011; 120:S225–S237. [PubMed: 21177775]

Aubrecht J, Caba E. Gene expression profile analysis: an emerging approach to investigate mechanisms of genotoxicity. Pharmacogenomics. 2005; 6:419–428. [PubMed: 16004560]

Auerbach O, Garfinkel L, Parks VR. Scar cancer of the lung: increase over a 21 year period. Cancer. 1979; 43:636–642. [PubMed: 217523]

Bushel PR, Heinloth AN, Li J, Huang L, Chou JW, Boorman GA, Malarkey DE, Houle CD, Ward SM, Wilson RE, Fannin RD, Russo MW, Watkins PB, Tennant RW, Paules RS. Blood gene expression signatures predict exposure levels. Proc Natl Acad Sci U S A. 2007; 104:18211–18216. [PubMed: 17984051]

Calvano SE, Xiao W, Richards DR, Felciano RM, Baker HV, Cho RJ, Chen RO, Brownstein BH, Cobb JP, Tschoeke SK, Miller-Graziano C, Moldawer LL, Mindrinos MN, Davis RW, Tompkins RG, Lowry SF. A network-based analysis of systemic inflammation in humans. Nature. 2005; 437:1032–1037. [PubMed: 16136080]

Coultas L, Strasser A. The role of the Bcl-2 protein family in cancer. Semin Cancer Biol. 2003; 13:115–123. [PubMed: 12654255]

Donaldson K, Aitken R, Tran L, Stone V, Duffin R, Forrest G, Alexander A. Carbon nanotubes: a review of their properties in relation to pulmonary toxicology and workplace safety. Toxicological Sciences. 2006; 92:5–22. [PubMed: 16484287]

Elgrabli D, Floriani M, Abella-Gallart S, Meunier L, Gamez C, Delalain P, Rogerieux F, Boczkowski J, Lacroix G. Biodistribution and clearance of instilled carbon nanotubes in rat lung. Part Fibre Toxicol. 2008; 5:20. [PubMed: 19068117]

Elliott RL, Blobe GC. Role of transforming growth factor Beta in human cancer. J Clin Oncol. 2005; 23:2078–2093. [PubMed: 15774796]

Garrett SH, Phillips V, Somji S, Sens MA, Dutta R, Park S, Kim D, Sens DA. Transient induction of metallothionein isoform 3 (MT-3), c-fos, c-jun and c-myc in human proximal tubule cells exposed to cadmium. Toxicol Lett. 2002; 126:69–80. [PubMed: 11738272]

Guo L, Ma Y, Ward R, Castranova V, Shi X, Qian Y. Constructing molecular classifiers for the accurate prognosis of lung adenocarcinoma. Clinical Cancer Research. 2006; 12:3344–3354. [PubMed: 16740756]

Guo NL, Wan YW, Tosun K, Lin H, Msiska Z, Flynn DC, Remick SC, Vallyathan V, Dowlati A, Shi X, Castranova V, Beer DG, Qian Y. Confirmation of gene expression-based prediction of survival in non-small cell lung cancer. Clinical Cancer Research. 2008; 14:8213–8220. [PubMed: 19088038]

Hironaka M, Fukayama M. Pulmonary fibrosis and lung carcinoma: a comparative study of metaplastic epithelia in honeycombed areas of usual interstitial pneumonia with or without lung carcinoma. Pathol Int. 1999; 49:1060–1066. [PubMed: 10632926]

Jagirdar J, Lee TC, Reibman J, Gold LI, Aston C, Begin R, Rom WN. Immunohistochemical localization of transforming growth factor beta isoforms in asbestos-related diseases. Environ Health Perspect. 1997; 105(Suppl 5):1197–1203. [PubMed: 9400723]

Karlsson HL, Cronholm P, Gustafsson J, Moller L. Copper oxide nanoparticles are highly toxic: a comparison between metal oxide nanoparticles and carbon nanotubes. Chem Res Toxicol. 2008; 21:1726–1732. [PubMed: 18710264]

Kim JE, Lim HT, Minai-Tehrani A, Kwon JT, Shin JY, Woo CG, Choi M, Baek J, Jeong DH, Ha YC, Chae CH, Song KS, Ahn KH, Lee JH, Sung HJ, Yu IJ, Beck GR Jr, Cho MH. Toxicity and clearance of intratracheally administered multiwalled carbon nanotubes from murine lung. J Toxicol Environ Health A. 2010; 73:1530–1543. [PubMed: 20954079]

Kobayashi N, Naya M, Ema M, Endoh S, Maru J, Mizuno K, Nakanishi J. Biological response and morphological assessment of individually dispersed multi-wall carbon nanotubes in the lung after intratracheal instillation in rats. Toxicology. 2010

Lam CW, James JT, McCluskey R, Hunter RL. Pulmonary toxicity of single-wall carbon nanotubes in mice 7 and 90 days after intratracheal instillation. Toxicological Sciences. 2004; 77:126–134. [PubMed: 14514958]

Livak KJ, Schmittgen TD. Analysis of relative gene expression data using real-time quantitative PCR and the 2(−Delta Delta C(T)) Method. Methods. 2001; 25:402–408. [PubMed: 11846609]

Long JM, Bell CW, Fagg WSt, Kushman ME, Becker KG, McCubrey JA, Farwell MA. Microarray and pathway analysis reveals decreased CDC25A and increased CDC42 associated with slow growth of BCL2 overexpressing immortalized breast cell line. Cell Cycle. 2008; 7:3062–3073. [PubMed: 18838868]

MacKinnon AC, Kopatz J, Sethi T. The molecular and cellular biology of lung cancer: identifying novel therapeutic strategies. Br Med Bull. 2010; 95:47–61. [PubMed: 20643690]

Mercer RR, Hubbs AF, Scabilloni JF, Wang L, Battelli LA, Schwegler-Berry D, Castranova V, Porter DW. Distribution and persistence of pleural penetrations by multi-walled carbon nanotubes. Part Fibre Toxicol. 2010; 7:28. [PubMed: 20920331]

Mercer RR, Hubbs AF, Scabolloni JF, Wang L, Battelli LA, Friend S, Castranova V, Porter DW. Pulmonary fibrotic resposne to aspiration of multi-walled carbon nanotubes. Particle Fibre Toxicol. 2011

Muller J, Decordier I, Hoet PH, Lombaert N, Thomassen L, Huaux F, Lison D, Kirsch-Volders M. Clastogenic and aneugenic effects of multi-wall carbon nanotubes in epithelial cells. Carcinogenesis. 2008; 29:427–433. [PubMed: 18174261]

Muller J, Huaux F, Moreau N, Misson P, Heilier JF, Delos M, Arras M, Fonseca A, Nagy JB, Lison D. Respiratory toxicity of multi-wall carbon nanotubes. Toxicol Appl Pharmacol. 2005; 207:221–231. [PubMed: 16129115]

Newton RK, Aardema M, Aubrecht J. The utility of DNA microarrays for characterizing genotoxicity. Environ Health Perspect. 2004; 112:420–422. [PubMed: 15033590]

Nuwaysir EF, Bittner M, Trent J, Barrett JC, Afshari CA. Microarrays and toxicology: the advent of toxicogenomics. Mol Carcinog. 1999; 24:153–159. [PubMed: 10204799]

Pacurari M, Castranova V, Vallyathan V. Single- and Multi-Wall Carbon Nanotubes Versus Asbestos: Are the Carbon Nanotubes a New Health Risk to Humans? Journal of Toxicology and Environmental Health-Part a-Current Issues. 2010; 73:378–395.

Peretz A, Checkoway H, Kaufman JD, Trajber I, Lerman Y. Silica, silicosis, and lung cancer. Isr Med Assoc J. 2006; 8:114–118. [PubMed: 16544735]

Pola R, Ling LE, Silver M, Corbley MJ, Kearney M, Blake Pepinsky R, Shapiro R, Taylor FR, Baker DP, Asahara T, Isner JM. The morphogen Sonic hedgehog is an indirect angiogenic agent upregulating two families of angiogenic growth factors. Nat Med. 2001; 7:706–711. [PubMed: 11385508]

Poland CA, Duffin R, Kinloch I, Maynard A, Wallace WAH, Seaton A, Stone V, Brown S, MacNee W, Donaldson K. Carbon nanotubes introduced into the abdominal cavity of mice show asbestos-like pathogenicity in a pilot study. Nature Nanotechnology. 2008; 3:423–428.

Porter D, Sriram K, Wolfarth M, Jefferson A, Schwegler-Berry D, Andrew M, Castranova V. A biocompatible medium for nanoparticle dispersion. Nanotoxicology. 2008; 2:144–154.

Porter DW, Hubbs AF, Mercer RR, Wu N, Wolfarth MG, Sriram K, Leonard S, Battelli L, Schwegler-Berry D, Friend S, Andrew M, Chen BT, Tsuruoka S, Endo M, Castranova V. Mouse pulmonary dose-and time course-responses induced by exposure to multi-walled carbon nanotubes. Toxicology. 2010; 269:136–147. [PubMed: 19857541]

Ryman-Rasmussen JP, Cesta MF, Brody AR, Shipley-Phillips JK, Everitt JI, Tewksbury EW, Moss OR, Wong BA, Dodd DE, Andersen ME, Bonner JC. Inhaled carbon nanotubes reach the subpleural tissue in mice. Nat Nanotechnol. 2009; 4:747–751. [PubMed: 19893520]

Sakai S, Ono M, Nishio T, Kawarada Y, Nagashima A, Toyoshima S. Lung cancer associated with diffuse pulmonary fibrosis: CT-pathologic correlation. J Thorac Imaging. 2003; 18:67–71. [PubMed: 12700479]

Sargent LM, Reynolds SH, Hubbs AF, Benkovic SA, Lowry DT, Kashon ML, Siergrist KT, Mustovich J, Sturgeon JL, Burker KL, Dinu CZ. Understanding carbon nanotubes genotoxicity. The Toxicologist. 2011; 120:A59.

Service RF. Meeting. American Chemical Society. Raising a glass to health and nanotubes. Science. 1999; 285:2053–2055. [PubMed: 10523196]

Shi L, Campbell G, Jones WD, Campagne F, Wen Z, Walker SJ, Su Z, Chu TM, Goodsaid FM, Pusztai L, Shaughnessy JD Jr, Oberthuer A, Thomas RS, Paules RS, Fielden M, Barlogie B, Chen W, Du P, Fischer M, Furlanello C, Gallas BD, Ge X, Megherbi DB, Symmans WF, Wang MD, Zhang J, Bitter H, Brors B, Bushel PR, Bylesjo M, Chen M, Cheng J, Chou J, Davison TS, Delorenzi M, Deng Y, Devanarayan V, Dix DJ, Dopazo J, Dorff KC, Elloumi F, Fan J, Fan S, Fan X, Fang H, Gonzaludo N, Hess KR, Hong H, Huan J, Irizarry RA, Judson R, Juraeva D, Lababidi S, Lambert CG, Li L, Li Y, Li Z, Lin SM, Liu G, Lobenhofer EK, Luo J, Luo W, McCall MN, Nikolsky Y, Pennello GA, Perkins RG, Philip R, Popovici V, Price ND, Qian F, Scherer A, Shi T, Shi W, Sung J, Thierry-Mieg D, Thierry-Mieg J, Thodima V, Trygg J, Vishnuvajjala L, Wang SJ, Wu J, Wu Y, Xie Q, Yousef WA, Zhang L, Zhang X, Zhong S, Zhou Y, Zhu S, Arasappan D, Bao W, Lucas AB, Berthold F, Brennan RJ, Buness A, Catalano JG, Chang C, Chen R, Cheng Y, Cui J, et al. The MicroArray Quality Control (MAQC)-II study of common practices for the development and validation of microarray-based predictive models. Nat Biotechnol. 2010; 28:827–838. [PubMed: 20676074]

Shiels MS, Albanes D, Virtamo J, Engels EA. Increased risk of lung cancer in men with tuberculosis in the alpha-tocopherol, Beta-carotene cancer prevention study. Cancer Epidemiol Biomarkers Prev. 2011; 20:672–678. [PubMed: 21335509]

Shukla A, Gulumian M, Hei TK, Kamp D, Rahman Q, Mossman BT. Multiple roles of oxidants in the pathogenesis of asbestos-induced diseases. Free Radic Biol Med. 2003; 34:1117–1129. [PubMed: 12706492]

Shvedova AA, Kisin ER, Mercer R, Murray AR, Johnson VJ, Potapovich AI, Tyurina YY, Gorelik O, Arepalli S, Schwegler-Berry D, Hubbs AF, Antonini J, Evans DE, Ku BK, Ramsey D, Maynard A, Kagan VE, Castranova V, Baron P. Unusual inflammatory and fibrogenic pulmonary responses to

single-walled carbon nanotubes in mice. Am J Physiol Lung Cell Mol Physiol. 2005; 289:L698–708. [PubMed: 15951334]

Stanton MF, Layard M, Tegeris A, Miller E, May M, Morgan E, Smith A. Relation of particle dimension to carcinogenicity in amphibole asbestoses and other fibrous minerals. J Natl Cancer Inst. 1981; 67:965–975. [PubMed: 6946253]

Sun M, Wang G, Paciga JE, Feldman RI, Yuan ZQ, Ma XL, Shelley SA, Jove R, Tsichlis PN, Nicosia SV, Cheng JQ. AKT1/PKBalpha kinase is frequently elevated in human cancers and its constitutive activation is required for oncogenic transformation in NIH3T3 cells. Am J Pathol. 2001; 159:431–437. [PubMed: 11485901]

Takagi A, Hirose A, Nishimura T, Fukumori N, Ogata A, Ohashi N, Kitajima S, Kanno J. Induction of mesothelioma in p53+/− mouse by intraperitoneal application of multi-wall carbon nanotube. Journal of Toxicological Sciences. 2008; 33:105–116. [PubMed: 18303189]

Takita M, Arisaka K, Kajita T, Kifune T, Koshiba M, Miyano K, Nakahata M, Oyama Y, Sato N, Suda T, Suzuki A, Takahashi K, Totsuka Y. Search for neutron-antineutron oscillation in 16O nuclei. Phys Rev D Part Fields. 1986; 34:902–904. [PubMed: 9957226]

Tian F, Cui D, Schwarz H, Estrada GG, Kobayashi H. Cytotoxicity of single-wall carbon nanotubes on human fibroblasts. Toxicol In Vitro. 2006; 20:1202–1212. [PubMed: 16697548]

Toonkel RL, Borczuk AC, Powell CA. Tgf-beta signaling pathway in lung adenocarcinoma invasion. J Thorac Oncol. 2010; 5:153–157. [PubMed: 20101143]

Vallyathan V, Green F, Ducatman B, Schulte P. Roles of epidemiology, pathology, molecular biology, and biomarkers in the investigation of occupational lung cancer. J Toxicol Environ Health B Crit Rev. 1998; 1:91–116. [PubMed: 9650532]

Vancheri C, Failla M, Crimi N, Raghu G. Idiopathic pulmonary fibrosis: a disease with similarities and links to cancer biology. Eur Respir J. 2010; 35:496–504. [PubMed: 20190329]

Vaslet CA, Messier NJ, Kane AB. Accelerated progression of asbestos-induced mesotheliomas in heterozygous p53+/− mice. Toxicol Sci. 2002; 68:331–338. [PubMed: 12151629]

Wan YW, Sabbagh E, Raese R, Qian Y, Luo D, Denvir J, Vallyathan V, Castranova V, Guo NL. Hybrid models identified a 12-gene signature for lung cancer prognosis and chemoresponse prediction. Plos One. 2010:5.

Wikman H, Ruosaari S, Nymark P, Sarhadi VK, Saharinen J, Vanhala E, Karjalainen A, Hollmen J, Knuutila S, Anttila S. Gene expression and copy number profiling suggests the importance of allelic imbalance in 19p in asbestos-associated lung cancer. Oncogene. 2007; 26:4730–4737. [PubMed: 17297452]

Yu YY, Pinsky PF, Caporaso NE, Chatterjee N, Baumgarten M, Langenberg P, Furuno JP, Lan Q, Engels EA. Lung cancer risk following detection of pulmonary scarring by chest radiography in the prostate, lung, colorectal, and ovarian cancer screening trial. Arch Intern Med. 2008; 168:2326–2332. discussion 2332. [PubMed: 19029496]

Zhu L, Chang DW, Dai L, Hong Y. DNA damage induced by multiwalled carbon nanotubes in mouse embryonic stem cells. Nano Lett. 2007; 7:3592–3597. [PubMed: 18044946]

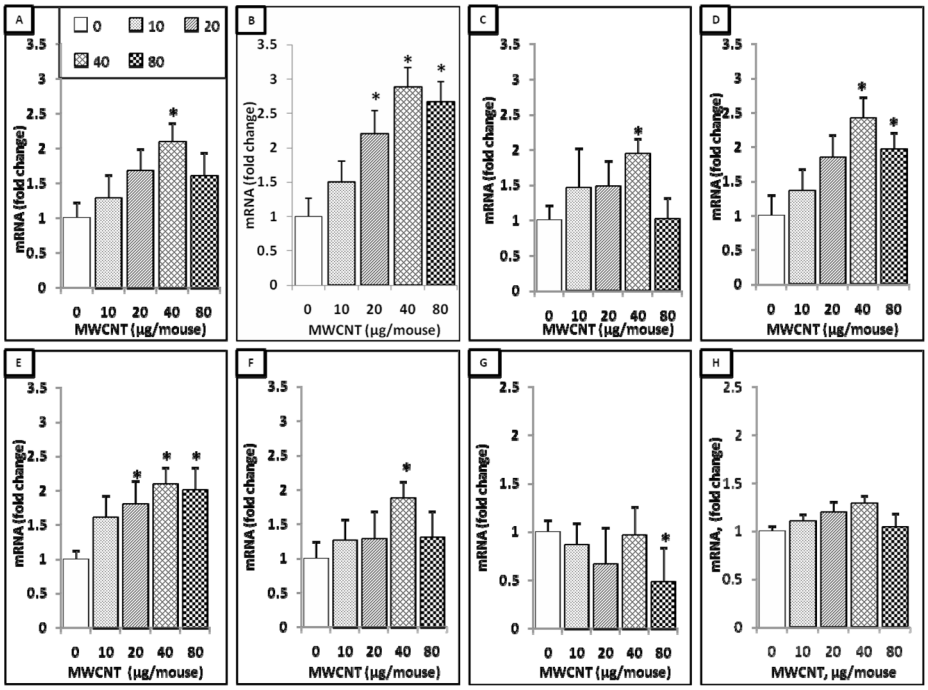

Figure 1.

7-gene biomarker set in the mouse lung at 7 days post-exposure to MWCNT. Total RNA was extracted from the frozen lung tissue of mice that were exposed to different doses of MWCNT at 7 days post-exposure as indicated, followed by cDNA generation. Real-time PCR was performed to profile 63 lung cancer biomarker genes using LDA. Genes shown in the figure underwent significant changes in expression when compared to the negative control. A, *Arhgap19*. B, *Ccdc99*. C, *Msx2*. D, *Mt3*. E, *Nos2*. F, *Shh*. G, *Wif1*. H, *18S*. Fold change was calculated after normalization to 18S and relative to control samples. Values given are mean ± SEM ($p \leq 0.05$, n=8). * significantly different compared to control (unpaired *t*-tests).

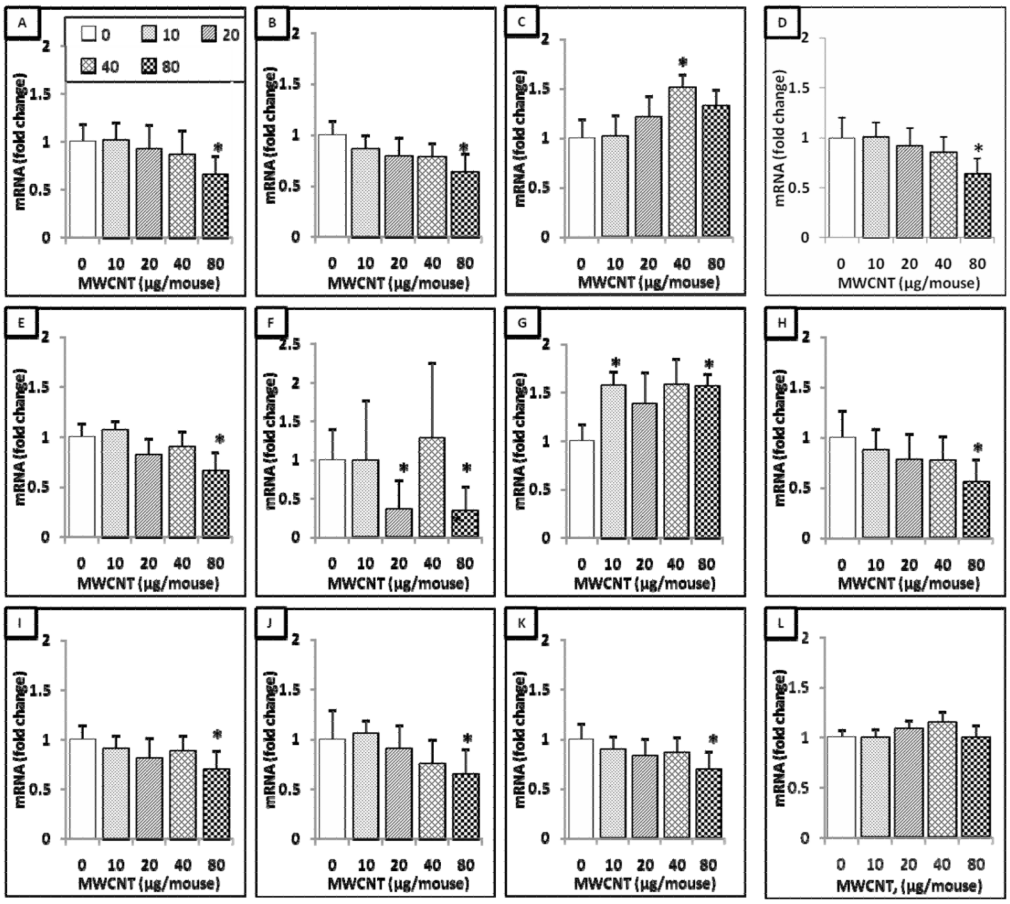

Figure 2.

11-gene biomarker set in the mouse lung at 56 days post-exposure to MWCNT. Total RNA was extracted from the frozen stored lung tissue of mice that were exposed to different doses of MWCNT at 56 days post-exposure as indicated, followed by cDNA generation. Real-time PCR was performed to profile 63 lung cancer biomarker genes using LDA. Genes shown in the figure underwent significant changes in expression when compared to the negative control. A, *Bcl2*. B, *Cav1*. C, *Ccdc99*. D, *Dhh*. E, *Gpx3*. F, *Msx2*. G, *Nos2*. H, *Pi3kr1*. I, *Ptch1*. J, *Wif1*. K, *Zak*. L, *18S*. Fold change was calculated after normalization to 18S and relative to control samples. Values given are mean ± SEM ($p \leq 0.05$, n=8). * significantly different compared to control (unpaired *t*-tests).

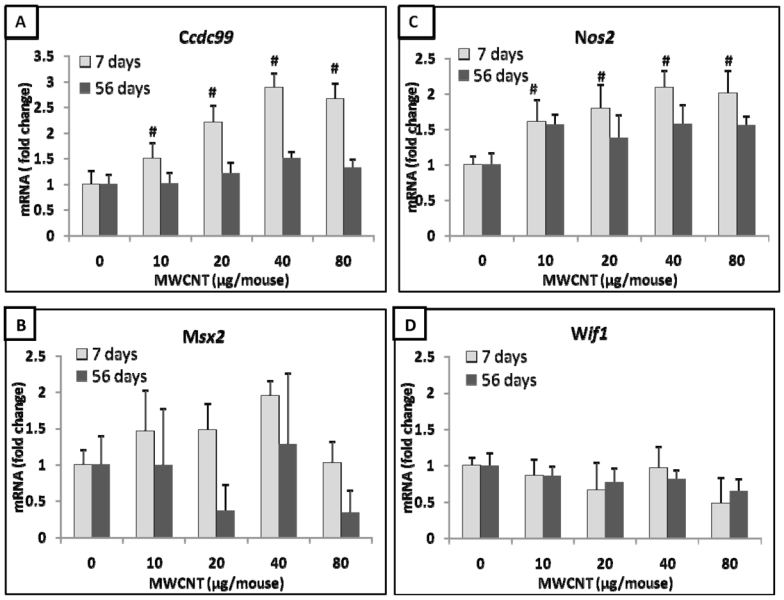

Figure 3.

An overlapping 4-gene biomarker set in the mouse lung between 7- and 11-gene set at 7 and 56 days post-exposure to MWCNT, respectively. A, *Ccdc99*. B, *Msx2*. C, *Nos2*. D, *Wif1*. Fold change was calculated after normalization to 18S and relative to control samples. Values given are mean ± SEM ($p \leq 0.05$, n=8). # significantly different compared to 56 days post-exposure.

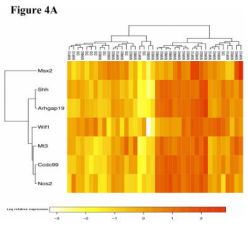

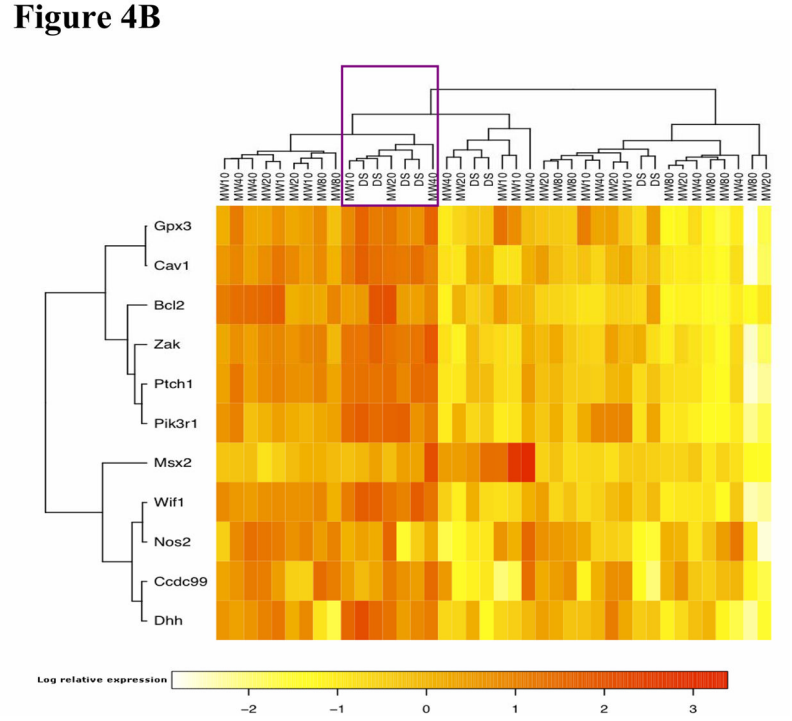

Figure 4.

Hierarchical clustering analysis. DS: control animal. The number after “MW” denotes the dosage used in the treatment. (A) Clustering analysis using the 7-gene biomarker set at 7 days post-exposure. (B) Clustering analysis using the 11-gene biomarker set at 56 days post-exposure. The marked cluster contains 4 control samples.

Figure 5A

7-gene biomarker set network analysis (7-day)

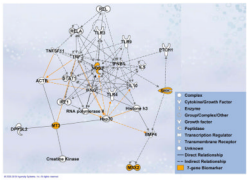

Figure 5B

11-gene biomarker set network analysis (56-day)

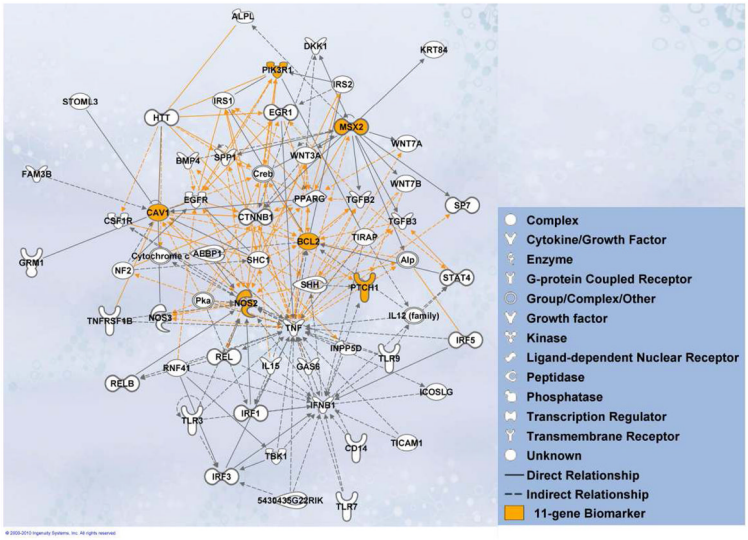

Figure 5.

Molecular network analysis using IPA. (A). Network associated with the 7-gene biomarker set identified from animals treated with MWCNT at 7 days post-exposure. (B). Network associated with the 11-gene biomarker set identified from animals treated with MWCNT at 56 days post-exposure.

Figure 6A

Top 5 significant canonical pathways in the 7-gene set network (7-day)

Ingenuity Canonical Pathways	Genes	P-value
Corticotropin Releasing Hormone Signaling	NOS2, PTCH1, SHH	9.55E-04
Role of Macrophages, Fibroblasts, and Endothelial Cells in Rheumatoid Arthritis	IL10, NOS2, RELA, TLR3, TLR4, TLR9, TNF, TNFSF11	7.94E-03
Sonic Hedgehog Signaling	PTCH1, SHH	1.26E-02
MIF Regulation of Innate Immunity	NOS2, RELA, TLR4	1.66E-02
MSP-RON Signaling Pathway	ACTB, IFNG, NOS2, TLR4, TNF	1.91E-02

Figure 6B

Top 5 significant canonical pathways in the 11-gene set network (56-day)

Ingenuity Canonical Pathways	Genes	*P*-value
Molecular Mechanisms of Cancer	BCL2, BMP4, CTNNB1, Cytochrome c, IRS1, PIK3R1, Pka, PTCH1, SHC1, SHH, TGFB2, TGFB3	6.92E-05
Docosahexaenoic Acid (DHA) Signaling	BCL2, Cytochrome c, PIK3R1	3.89E-04
Role of Osteoblasts, Osteoclasts, and Chondrocytes in Rheumatoid Arthritis	Alp, ALPL, BCL2, BMP4, CSF1R, CTNNB1, DKK1, PIK3R1, SP7, SPP1, TNF, TNFRSF1B, WNT3A, WNT7A, WNT7B	4.37E-04
MSP-RON Signaling Pathway	IL12 (family), NOS2, PIK3R1, TNF	4.47E-04
Glucocorticoid Receptor Signaling	BCL2, Creb, NOS2, PIK3R1, Pka, SHC1, TGFB2, TGFB3, TNF	6.61E-04

Figure 6C

Comparison of canonical pathways in 7- and 11-gene set networks

	7-gene network	11-gene network
number of canonical pathways	25	154
number of significant (*P* <0.05) canonical pathways	13	81
number of common significant canonical pathways	**12**	

12 significant pathways common to both 7- and 11-gene biomarker networks

Ingenuity Canonical Pathways	*P*-value (in 7-gene network)	*P*-value (in 11-gene network)
Basal Cell Carcinoma Signaling	0.0309	0.0513
Corticotropin Releasing Hormone Signaling	0.000955	0.00282
HIF1 Signaling	0.0447	0.00245
IL-12 Signaling and Production in Macrophages	0.0437	0.00240
IL-17 Signaling	0.0324	0.00129
LXR/RXR Activation	0.0295	0.0490
MIF Regulation of Innate Immunity	0.0166	0.0275
MSP-RON Signaling Pathway	0.0191	0.000447
Relaxin Signaling	0.0537	0.00363
Role of Macrophages, Fibroblasts and Endothelial Cells in Rheumatoid Arthritis	0.00794	0.00138
Sonic Hedgehog Signaling	0.0126	0.0209
Type I Diabetes Mellitus Signaling	0.0457	0.00257

Figure 6D

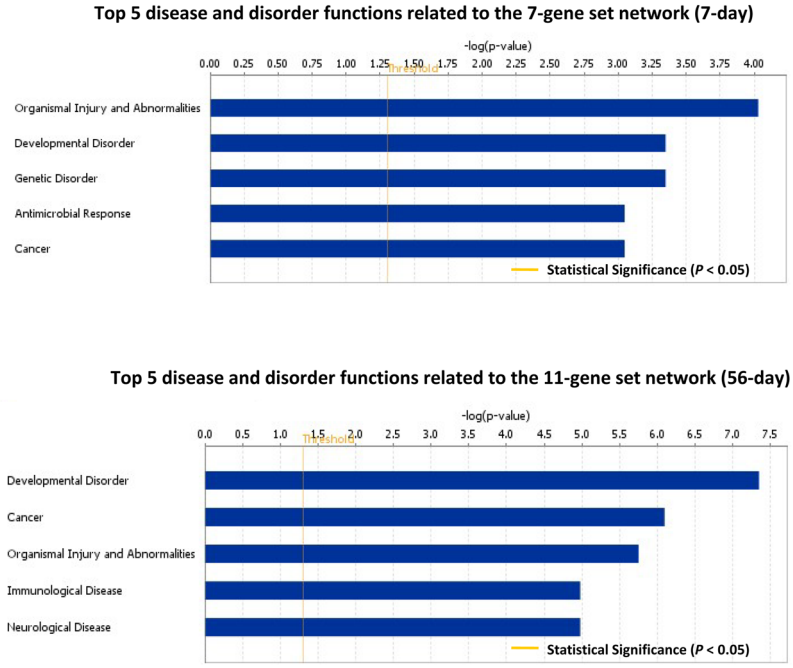

Figure 6.

Canonical pathways, diseases and functional disorders related to the networks generated from the 7- and 11-gene biomarker sets using IPA. (A). Canonical pathway analysis in the network related to the 7-gene biomarker set. (B). Canonical pathway analysis in the network related to the 11-gene biomarker set. (C). Comparison of canonical pathways in the 7- and

11-gene biomarker set network analysis. (D). Top 5 disease and disorder functions related to the 7-gene biomarker set network (at 7 day post-exposure) and the 11-gene biomarker set network (at 56 day post-exposure).

Table 1

Information for the 63 genes analyzed in this study.

Gene Symbol	Gene name	Assay ID	Function	Pathways	Remarks
Ahnak	Desmoyokin	Mm00613028_m1	Protein:protein binding	Signal transduction	Prognostic maker for lung cancer (Guo *et al.*, 2006; Guo *et al.*, 2008)
Akt1	Protein kinase B subunit alpha	Mm01331624_m1	Kinase activity	Signal transduction	Oncogen2 ((Sun *et al.*, 2001)
Arhgap19	Rho GTPase activating protein-19	Mm01198653_m1	GTPase activity	Signal transduction	Prognostic maker for lung cancer (Guo *et al.*, 2006; Guo *et al.*, 2008)
Arhgdig	Rho-related GDP- dissociation inhibitor	Mm00433576_m1	Cell signaling protein	Signal transduction	Prognostic maker for lung cancer (Guo *et al.*, 2006; Guo *et al.*, 2008)
Atp5a1	ATP synthase alpha- subunit-1	Mm00431960_m1	Atpase, hydrogen- transporting, ATP synthase activity		Prognostic maker for lung cancer (Guo *et al.*, 2006; Guo *et al.*, 2008)
Atp6v0d1	vacuolar (V−) ATPase proton pump subunit D1	Mm00442694_m1	Atpase H+-exporting	Organelles acidification	Prognostic maker for lung cancer (Wan *et al.*, 2010)
Atp8a2	P4-type ATPases or Phosphatidylserine Flippase	Mm00443740_m1	Atpase, negative regulation of cell proliferation, aminophospholipid transport	Transport across membranes	Prognostic maker for lung cancer (Guo *et al.*, 2006; Guo *et al.*, 2008)
Atrx	Alpha thalassemia/mental retardation syndrome X- linked	Mm01225442_m1	Transcriptional regulator, chromatin remodeling	Transcription	Prognostic maker for lung cancer (Guo *et al.*, 2006; Guo *et al.*, 2008)
Bcl2	B-cell leukemia/lymphoma-2	Mm00477631_m1	Protein binding, anti-apoptosis	Signal transduction	
Cav1	Caveolin-1	Mm00483057_m1	Vasculogenesis, endocytosis		Tumor suppressor gene candidate
Ccdc99	Coiled-coil domain containing −99	Mm00510371_m1	Establishment of mitotic spindle orientation	Cell cycle	Prognostic marker for lung cancer (Wan *et al.*, 2010)
Chd4	Chromodomain helicase DNA binding protein-4	Mm01190896_m1	Transcription regulator	Transcription	Prognostic maker for lung cancer (Guo *et al.*, 2006; Guo *et al.*, 2008)
Cox2	Prostaglandin G/H synthase-2	Mm01307329_m1	Inflammation, mitogenesis	Signal transduction	
Creb3	cAMP responsive element binding protein 3	Mm00457268_m1	Transcription factor	Transcription	Prognostic maker for lung cancer (Guo *et al.*, 2006; Guo *et al.*, 2008)
Dhh	Deserted hedgehog	Mm01310203_m1	Protein binding, peptidase activity, cell-cell signaling	Signal transduction	

Gene Symbol	Gene name	Assay ID	Function	Pathways	Remarks
Dlc1	Deleted in liver cancer-1	Mm00507957_m1	GTPase activity	Signal transduction	A candidate tumor suppressor gene; Prognostic marker for lung cancer (Wan *et al.*, 2010)
E2f4	E2F transcription factor-4	Mm00514160_m1	Transcriptional factor, cell cycle apoptosis	Transcription	Prognostic maker for lung cancer (Guo *et al.*, 2006; Guo *et al.*, 2008)
Egf	Epidermal growth factor	Mm01316968_m1	Growth factor	Signal transduction	Oncogene; Prognostic maker for lung cancer (Guo *et al.*, 2006; Guo *et al.*, 2008)
Erk1/Mapk 3	Extracellular signal- regulated kinase-1	Mm00662375_g1	Serine/threonine kinase activity	Signal transduction	
Erk2/Mapk1	Extracellular signal- regulated kinase-2	Mm00442479_m1	Serine/threonine kinase activity	Signal transduction	
Fam164A	Family with sequence similarity 164, member A	Mm00557410_m1	Unknown	Unknown	Prognostic marker for lung cancer (Wan *et al.*, 2010)
Fut7	Fucosyltransferase-7	Mm01330673_g1	Protein glycosylation	Metabolism	Prognostic maker for lung cancer (Guo *et al.*, 2006; Guo *et al.*, 2008)
Gli1	Glioma-associated oncogene homolog -1	Mm00494645_m1	DNA, protein binding	Transcription	
Gnb1	Guanine nucleotide binding protein (G protein), beta polypeptide -1.	Mm00515002_m1	GTPase activity	Signal transduction	
Gpx3	Plasma gluthatione peroxidase-3	Mm00492427_m1	Response to oxidative stress	Antioxidant activity	
HnrnpA3	Heterogeneous nuclear ribonucleoprotein-A3	Mm00817148_g1	mRNA binding, protein binding	Signal transduction	Prognostic maker for lung cancer (Guo *et al.*, 2006; Guo *et al.*, 2008)
Igl-v1	Immunoglobulin lambda variable 1–44	Mm01611614_m1	Signaling in immune system	Immunity	Prognostic maker for lung cancer (Guo *et al.*, 2006; Guo *et al.*, 2008)
Ihh	Indian hedgehog	Mm01259021_m1	Development processes	Signal transduction	
Ilf3	Interleukin enhancer- binding factor-3	Mm00494960_m1	DNA, protein binding	Transcription	Prognostic maker for lung cancer (Guo *et al.*, 2006; Guo *et al.*, 2008)
Insr	Insulin receptor	Mm01211875_m1	Growth factor receptor, insulin receptor	Signal transduction	Oncogene; Prognostic maker for lung cancer (Guo *et al.*, 2006; Guo *et al.*, 2008)
Lmf1	Lipase maturation factor-1	Mm00512942_m1	Maturation of specific proteins in ER, transport of lipoprotein lipase	Protein transport	Prognostic marker for lung cancer (Wan *et al.*, 2010)
Mark2	MAP/microtubule affinity-regulating kinase-2	Mm00433039_m1	Serine/threonin kinase activity	Signal transduction	Prognostic maker for lung cancer (Guo *et al.*, 2006; Guo *et al.*, 2008)

Gene Symbol	Gene name	Assay ID	Function	Pathways	Remarks
Msx2	Muscle segment homeobox gene-2	Mm00442992_m1	Transcription suppressor genes	Transcription	Prognostic maker for lung cancer (Guo *et al.*, 2006; Guo *et al.*, 2008)
Mt3	Metallothionin-3	Mm00496661_g1	Cellular metal ion homeostasis, removal of superoxide radicals, binds to heavy metals	Antioxidant activity	Oncogene; Prognostic maker for lung cancer (Guo *et al.*, 2006; Guo *et al.*, 2008)
Nos1	Nitric oxide synthase-1	Mm00435175_m1	Nitric oxide synthesis, neurotransmiter	Signal transduction	
Nos2	Nitric oxide synthase-2	Mm00440488_m1	Response to hypoxia; positive regulation of leukocyte mediated cytotoxicity, endothelial cell proliferation, blood vessel remodeling, nitric oxide synthesis	Signal transduction	Biomarker for bronchopulmonary dysplasia
Nos3	Nitric oxide syntahse-3	Mm01164908_m1	Nitric oxide synthesis, diverse biological functions	Signal transduction	Biomarker for prostatic carcinoma
Nsfl	N-ethylmaleimide- sensitive factor	Mm01243864_g1	Vesicle transport/target membrane fusion	Cellular transport	
Ogt	O-linked N- acetylglucosamine (GlcNAc) transferase	Mm00507317_m1	Glycosilation	Metabolism	Prognostic maker for lung cancer (Guo *et al.*, 2006; Guo *et al.*, 2008)
Pdpk1	Pyruvate dehydrogenase kinase, isozyme-1	Mm00440707_m1	Protein kinase activity	Signal transduction	Oncogene, Prognostic marker for lung cancer (Wan *et al.*, 2010)
Pik3r1	Phosphoinositide-3- kinase, regulatory subunit-1 (alpha)	Mm00803160_m1	Protein localization in plasma membrane	Signal transduction	
Prmt1	Protein arginine methyltransferase-1	Mm00480133_m1	Tranferease histone methyltransferase	Signal transduction	Prognostic maker for lung cancer (Guo *et al.*, 2006; Guo *et al.*, 2008)
Ptch1	Patched-1	Mm00436014_m1	Receptor activity	Signal transduction	Tumor suppressor gene
Rer1	Retention in endoplasmic reticulum-1	Mm00471276_m1	Endoplasmic reticulum membrane proteins	Protein retention in ER	Prognostic maker for lung cancer (Guo *et al.*, 2006; Guo *et al.*, 2008)
Scly	Selenocysteine lyase	Mm00489563_m1	Catalyzes the decomposition of L-selenocysteine	Metabolism	Prognostic marker (Wan *et al.*, 2010)
Shh	Sonic hedgehog	Mm00436527_m1	Proliferation, differentiation, development, specification, signaling, survival, migration, growth	Signal transduction	
Smo	Smoothened	Mm01162710_m1	Signal transducer	Signal transduction	
Smpd1	Sphingomyelin phosphodiesterase-1, acid lysosomal	Mm00488318_m1	Converts sphingomyelin to ceramide	Metabolism	Prognostic marker for lung cancer (Wan *et al.*, 2010)
Sod1	Superoxide dismutase-1	Mm01344231_g1	Oxidative stress response	Antioxidant signaling	
Sod2	Superoxide dismutase-2	Mm00449726_m1	Oxidative stress response	Antioxidant signaling	

Gene Symbol	Gene name	Assay ID	Function	Pathways	Remarks
Sod3	Superoxide dismutase-3	Mm00448831_s1	Oxidative stress response, xenobiotic metabolism signaling	Antioxidant signaling	
Stk24	Serine/threonine kinase- 24	Mm00520930_m1	Protein kinase activity	Signal transduction	Prognostic marker for lung cancer (Wan *et al.*, 2010)
Tal2	T-cell acute lymphocytic leukemia-2	Mm00447439_s1	DNA, and protein binding factor	Transcription regulation	T cell acute lymphoblastic leukemia.Oncogene; Prognostic maker for lung cancer (Guo *et al.*, 2006; Guo *et al.*, 2008)
Tnfsf9	Tumor necrosis factor (ligand) superfamily, member-9	Mm00437154_m1	Bidirectional signal transducer	Signal transduction	Oncogene; Prognostic maker for lung cancer (Guo *et al.*, 2006; Guo *et al.*, 2008)
Tuba1a	Tubulin, alpha-1a	Mm00846967_g1	Microtubule- based movement, protein polymerization	Structural activity	Prognostic maker for lung cancer (Guo *et al.*, 2006; Guo *et al.*, 2008)
Uba1	Ubiquitin-like modifier activating enzyme-1	Mm00493988_m1	Ubiquitin- conjugation for protein degradation	Protein degradation	Prognostic maker for lung cancer (Guo *et al.*, 2006; Guo *et al.*, 2008)
Ube2i	Ubiquitin-conjugating enzyme E2I	Mm00495850_m1	Ubiquitin- activating protein	Protein degradation	Prognostic maker for lung cancer (Guo *et al.*, 2006; Guo *et al.*, 2008)
Vac14	Protein Vac14 homolog	Mm00461494_m1	Regulates the level of PtdIns(3,5) P2	Signal transduction	Prognostic maker for lung cancer (Guo *et al.*, 2006; Guo *et al.*, 2008)
Vegfa	Vascular endothelial growth factor A	Mm01281449_m1	Angiogenesis	Signal transduction	
Wif1	WNT inhibitory factor-1	Mm00442355_m1	Development, Wnt receptor signaling pathway	Signal transduction	Tumor suppressor gene
Wnt3a	Wingless-type MMTV integration site family, member-3A	Mm00437337_m1	Protein binding, extracellular matrix structural constituent	Signal transduction	Oncogene
Xpo1	Exportin-1	Mm00506129_m1	Protein transporter activity	Protein transport	Prognostic marker for lung cancer (Wan *et al.*, 2010)
Zak	Leucine zipper- and sterile alpha motif-containing kinase	Mm00458198_m1	Protein kinase activity, cell cycle control	Signal transduction	Biomarker for diagnosis of cervical cancer; Prognostic marker for lung cancer (Wan *et al.*, 2010);. Oncogene
18S	18S ribosomal RNA		Protein synthesis		